Biomed Microdevices (2008) 10:631–638
DOI 10.1007/s10544-008-9174-7

Microfluidic high viability neural cell separation using viscoelastically tuned hydrodynamic spreading

Zhigang Wu · Klas Hjort · Grzegorz Wicher · Åsa Fex Svenningsen

Published online: 7 May 2008

Abstract A high viability microfluidic cell separation technique of high throughput was demonstrated based on size difference continuous mode hydrodynamic spreading with viscoelastic tuning. Using water with fluorescent dye as sample fluid and in parallel introducing as elution a viscoelastic biocompatible polymer solution of alginic sodium, the spreading behavior was investigated at different polymer concentrations and flow rates. Particle separation was studied in the same detail for 9.9 μm and 1.9 μm latex beads. Using buffered aqueous solutions and further surface treatments to protect from cell adhesion, separation between neuron cells and glial cells from rat's spine cord was demonstrated and compared to the separation of latex particles of 20 and 4.6 μm sizes. High relative viability (above 90%) of neural cells was demonstrated compared the reference cells of the same batch.

Keywords Microfluidics · Viscoelastic · Neural cell · Separation

1 Introduction

Recently, there has been a growing requirement of scientific world for isolation of specific populations of cells derived from nervous system. Cell type heterogeneity, biochemical complexity and extreme sensitivity for environmental changes (physical and chemical) make primary neural cells difficult to manipulate. Therefore, high viability of sorted cells plays a crucial role in obtaining stable and reproducible *in vitro* system in order to understand their specific and unique functions in living systems (Davies et al. 2006; Jiang et al. 2006; Hedlund et al. 2007).

In the search for high throughput separation of cells by size in microfluidic systems, hydrodynamic spreading has shown promising results. However, to ease its use a tuning mechanism should be introduced. In this work we demonstrate a simple mechanism—viscoelastic tuning.

Microfluidics offers today a platform for cell study and total analysis systems, with high potential in the typical process including cell culture, treatment, selection, lysis, separation and analysis (El-Ali et al. 2006). Cell selection, sorting or separation is one of critical techniques in the microfluidic platform for cell study (Dittrich and Manz 2006). Various efforts have been put on the development of the cell sorting, both on mechanism and devices by miniaturization of the capillary fluidic macro device (Fu et al. 1999; Huh et al. 2003; Dittrich and Schwille 2003; Kurabayashi et al. 2003; and Zhang et al. 2005) or by utilizing unique microfluidic geometries (Yamada et al. 2004; Takagi et al. 2005; Yamada et al. 2007; Wu et al. 2007; Choi et al. 2007; Blom et al. 2003; Huang et al. 2004; Yang et al. 2006; Petersson et al. 2005; Pamme and Wilhelm 2006; Kang et al. 2007). Among the different kinds of methods, continuous cell separation is very interesting because of its potential high throughput and that it is ideal for combining with upstream and downstream application, hence making it easier to integrate it into more complex microfluidic systems and achieve truly micro total analysis systems (μTAS; Pamme 2007).

Z. Wu (✉) · K. Hjort
Department of Engineering Sciences, The Ångström Laboratory,
Uppsala University,
751 21 Uppsala, Sweden
e-mail: Zhigang.Wu@angstrom.uu.se

G. Wicher · Å. Fex Svenningsen
Department of Neuroscience, The Biomedical Center,
Uppsala University,
751 23 Uppsala, Sweden

Recently, microfluidic continuous cell separation based on hydrodynamic interaction with the microfluidic channel has attracted attention because of its robustness, potential high throughput and cell viability (Yamada et al. 2004; Takagi et al. 2005; Yamada et al. 2007; Wu et al. 2007; Choi et al. 2007). Here, we want to especially mention the work of Yamada et al.: By combining flow field flow fraction (Giddins 1993) and hydrodynamic spreading in the microchannel, a simple approach was demonstrated to separate particles based on size differences (Yamada et al. 2004; Takagi et al. 2005). Recently separation of liver cells was demonstrated (Yamada et al. 2007).

In hydrodynamic separation the tuning to certain particle sizes is made by adjusting the flow rate ratio. This is limited by the pump performance. In constant flow syringe pumping it is often limited by the syringe sizes. In constant pressure pumping (such as compressor) it is technically difficult to accurately adjust the tiny pressure difference in microfluidic applications. This makes it not convenient to control the flow and adjust to the particle size to separate. Combined with electroosmotic flow and pressure driven flow, we recently proposed an easy method to tune separations of different particle size ratios, with good results to more sturdy cells (Wu et al. 2007). However, many cells need a solution that will have too high ionic content, or they may be too sensitive to electric fields or currents, so that electroosmotic flow cannot be used.

Generally, many biocompatible polymer solutions can be added to cell containing fluids, which make the viscosity change with the shear rate. Sodium Alginate or alginic sodium, a polymer extracted from brown algae, is widely used in the food industry as a stabilizer. Recently, it has been used in microfluidic platform for cell manipulation due to its biocompatible, and being biodegradable to cells (Braschler et al. 2005). Also, sodium alginate can keep high cell viability even for very environmental sensitive mammalian cells such as liver cells (Wang et al. 2003). At the same time, as a polymer with its long chain, its aqueous solution shows a special character of polymer solutions—it is viscoelastic. That is, its viscosity will change with the changes of shear rate and this feature can be used to control and tune the hydrodynamic spreading simply by changing the flow rate. Viscoelastic is an interesting phenomena existing in fluid due to the elastic component of the liquid and it has also attracts the attention from the microfluidic community (Squires and Quake 2005), e.g. for mixing (Gan et al. 2006), focusing (Leshansky et al. 2007) and particle fractionation (Devarakonda et al. 2007). However, to our understanding this is the first study of viscoelasticity tuning of the hydrodynamic spreading in a microfluidic channel.

In this paper, our aim was to seek a robust high-throughput and simple microfluidic system that allows cell separation based on size for sensitive cells. For this the tuning effects of the viscoelastic phenomenon of aqueous polymer solutions in hydrodynamic spreading were studied and demonstrated in neural cells separation from glia cells at high cell viability. By using a highly biocompatible alginic sodium aqueous solution this novel viscoelastic tuning is not only simplifying separation by hydrodynamic spreading but is also allowing for high cell viability.

2 Separation and viscoelastical tuning mechanisms in hydrodynamic spreading

Normally, for Newtonian fluid such as water, the stress of the fluid is proportional to the shear rate. This constant rate is considered as the viscosity of the fluid. However, some solutions of larger molecular polymers have a different character. In contrary to small molecules such as water, normally these polymers have very long linear molecular chains. Due to the much larger length-to-diameter ratio, the shape and distribution of the polymers will change in the different liquid environments. For example, at no flow and hence no stress, to minimize the surface energy the polymers trend to curved and tangled together and the polymer solution shows high viscosity. However, when a stress is applied, the molecules are stretched in the stress/flow direction. The density of the molecules in the flow cross-section is decreased and the polymer solution shows lower viscosity. A simple model is to look on the molecule as two beads with a Hookean spring connection (Squires and Quake 2005). At the high shear rate the spring is stretched and at the low shear rate the spring is relaxed. The corresponding phenomena are that at high shear rate the polymer solution shows lower viscosity whereas at low shear rate it shows high viscosity. Therefore, when the channel shape and geometry are fixed, the viscosity will change with the flow rate of the fluid inside. In a previous work of one of the authors (Wu and Nguyen 2005), this phenomenon was shown to control the width of the sample stream. Hence, it can be used for cell separation, tuning the spreading behavior continuously inside a micro channel. With a constant ratio of the flow rate, the spreading behavior will be decided only by the viscosity or flow rate of the polymer flow, Fig. 1.

In the microfluidic device, the Reynolds number is small and resulting the laminar flow in the channel. With a syringe pump, the particle/cell suspension and another elution flow are primed in a microchannel by two syringes. Here, an aqueous polymer solution serves as an elution flow. Due to fixed syringes, the flow rate ratio of the two fluids is fixed, too. Thus, the spreading behavior of the two fluids is only decided by the flow rate of the two fluids. When the elution flow is at lower viscosity, the particle/cell suspension occupies a larger ratio of the whole channel

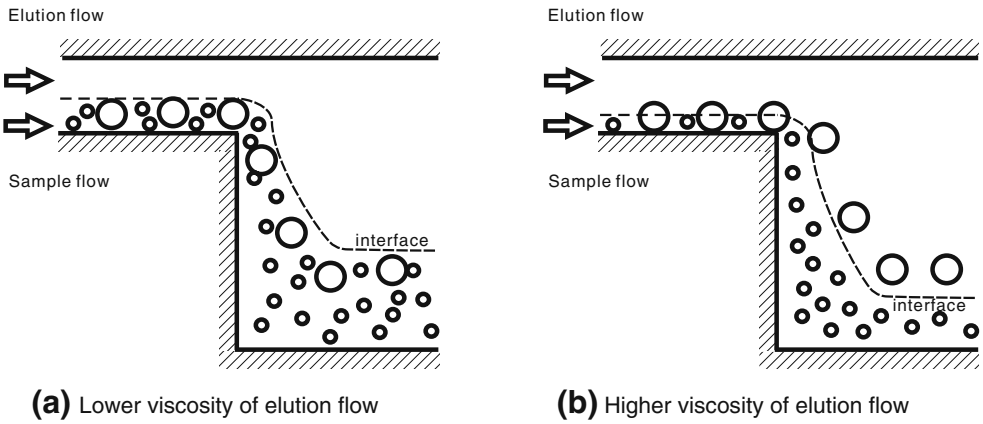

Fig. 1 Schematic of viscoelastically tuned hydrodynamic spreading for cell separation: (**a**) lower viscosity of elution flow and (**b**) higher viscosity of elution

width and both of the larger and smaller particles/cells are not aligned against the wall. The centers of the larger or small particle/cell are random distributed. The result is that their trajectories are overlapped and cannot be distinguished by hydrodynamic flow even if using an expanding channel, Fig. 1(a). However, when the elution flow is at higher viscosity, the particle/cell suspension occupies a smaller ratio of the whole channel width and the larger particles/cells are aligned against the wall (whereas the smaller particle/cells are aligned or not to the wall, which is dependant on the size ratio of the larger one and small one). The interface of the sample and elution flow will move towards the wall near sample flow, Fig. 1(b). Due to the large sizes, their centers of larger ones will be exposed into the elution fluid. In a laminar flow, for the round particle/cell, their trajectories of particle/cell are same to that of their centers. Using an expanding channel, or proper designed branch channel, the larger ones can be separated from the rest of the suspension, and collected in a corresponding collector.

3 Materials and methods

3.1 Chemicals and materials

For the microfluidic devices were used polydimethylsiloxane (PDMS) elastomer and cross linker, Elastosil RT601A and B, Wacker Chemie AG (München, Germany), and standard microscope glass slides ($26\times76\times1.0$ mm^3) from Menzel GmbH, Braunschweig, Germany. For the mould of the PDMS were used SU-8 2050 (epoxy-based negative photo-resist, MicroChem, Newton, MA) with developer (mr-Dev 600, micro resist technology, GmbH, Germany) and 4-in. silicon wafers.

The fluorescent dye used was fluorescein disodium salt $C_{20}H_{10}Na_2O_5$ (with commercial name Acid Yellow 73 or C.I. 45350) from Lancaster synthesis, UK. The maximum absorption of the dye occurs at a wavelength of 490 nm, while maximum emission occurs at the wavelength of 520 nm. The fluorescent dye was solved in DI water. To enhance the fluorescent intensity, sodium hydroxide was added to a pH 9. The low-viscosity aqueous solution was a sodium hydroxide, phosphate buffered saline (PBS, pH 7.4) buffer package supplied from Sigma-Aldrich, St Louis, MO, USA. For the polymer solution were used sodium alginate (very low viscosity), tris(hydroxymethylamino) methane (TRIS), and 2-(4-morpholino)ethanesulfonic acid (MES), and for surface treatment hydroxypropylcellulose (HPC; 100,000 MW), all from Alfa Aesar GmbH, Germany. The solvents acetone, methanol and iso-propanol were from Merck (Darmstadt, Germany). Suspensions with polystyrene latex microbead with diameters of 1.9 μm (green fluorescent dye), 4.6 μm (non fluorescent dye), 9.9 μm (green fluorescent dye) and 20 μm (non-fluorescent, white) were provided by Duke Scientific Corporation, CA, USA. To increase the stability of the diluted particles, polysorbate 20 (Tween 20, Alfa Aesar GmbH, Germany) was added.

To obtain dissociated mixed cultures from the spinal cord Leibovitz's L-15 medium (Invitrogen, Sweden) was used. Total and viable cell counts were using Trypan Blue (Sigma-Aldrich, Sweden) staining.

3.2 Fabrication of the SU-8 master

An SU-8 master was fabricated using a standard soft lithographic technique on a 4-in. silicon wafer (Xia and Whitesides 1998). A 40/164 μm thick layer of SU-8 2050 was spun on the silicon wafer, followed by soft baking, exposure to UV light through a CAD-designed chrome mask in a Karl Süss MA6/BA6 mask aligner and post-exposure baking according to the supplier's recipe. The channel network was developed and finally hard baked for 30 min at 150°C for complete adherence of the resist structure to the silicon wafer.

3.3 Fabrication of the prototype chip

A 10:1 (wt:wt) PDMS prepolymer and cross linker were mixed thoroughly by stirring and poured onto the SU-8 master. The mixture was put in a vacuum chamber for 15 min, and then in air for 1–2 h for degassing at the room temperature. Finally it was curing for 1 h at 70°C in an oven, and the PDMS replica was peeled off and holes were punched out for fluidic connects. The PDMS structure and the glass slide were activated using corona discharging (ETP, Chicago, IL, USA), by manually scanning the field-effect wire 3 to 5 mm above the surface at 15 s cm^{-2}. The components were joined together, and the bond was stabilized for 30 min at 70°C.

The device and its channel network are shown in Fig. 2. The entire channel network has a constant depth (height) of 40 μm. The two inlets are 3 mm long and 100 μm wide. The throat has a width of 30 μm and a length of 100 μm. The smaller collector channel has a width of 25 μm and the larger has a width of 500 μm. Both of them are 2.5 mm long.

3.4 Modification of the microchannel surface

An instant plasma treatment was used to modify the hybrid prototype. A corona sharp tip is inserted in the reservoirs for a few seconds, whereas an accumulated spark is created. The high voltage and high frequency spark migrated in the whole channel network, and rapidly oxidized the inner surface of the channel. This process makes the PDMS surface hydrophilic and highly negative charged. To protect cell adherences, after the plasma treatment the channel system was filled with 1.5% HPC dissolved inside MES/TRIS buffer (80 mM/40 mM; Sanders et al. 2003). The device was then put in a good seal container with high humidity environments and kept in a refrigerator at 6°C for overnight. Before cell separation, the device was flushed with sterile PBS buffer.

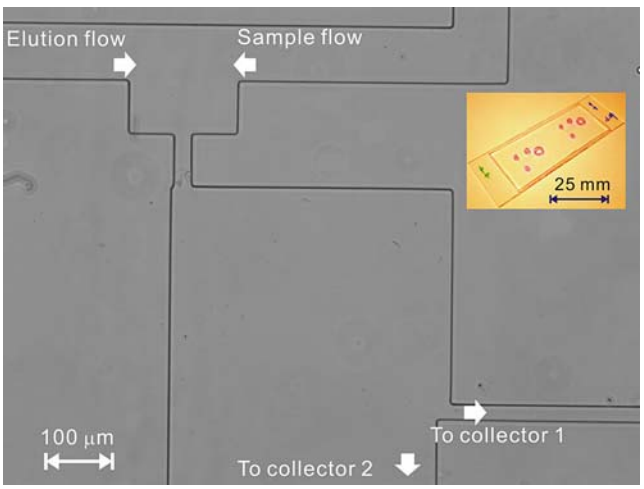

Fig. 2 The micrograph of the channel network and photo of the two devices on a glass slide

3.5 Instruments and spreading analysis

An inverted microscope with a set of epi-fluorescence attachment (Nikon TE2000-U, Japan) was used to observe the spreading behavior and monitor the particle tracking. For study of the spreading behavior, the image was captured using a high sensitive cooled CCD camera (Spot RL Mono, Diagnostic Instruments, MI, USA). The resolution of the camera is 1,600×1,200 pixels with 12-bit grayscale.

In the spreading measurement, DI water served as one fluid and fluorescent dye diluted in the alginate sodium solution as the other. Two gastight syringes (Hamilton, Switzerland) were filled with the two fluids and placed on a syringe pump (Harvard apparatus, PHD 2000, infusion). The observed area was illuminated with a 100 W mercury lamp. Among the measurements, an epi-fluorescent attachment of type Nikon B-2A was used (excitation filter for 450–490 nm, dichroic mirror for 505 nm and emission filter for 520 nm). The microscope was operated in the phase contrast mode to obtain a better contrast of the particles and cells.

After recording of the images onto the PC, the concentration profiles were evaluated using a self-developed program written in MATLAB as described previously (Wu et al. 2004). Subsequently, a path with the known position across the channel was evaluated. The position across the channel was normalized against the channel width, while the measured pixel intensity was normalized against the maximum and minimum intensities in the place where the two fluids just met. The spreading width or fraction was obtained at the location where the dimensionless intensity was 0.5.

For particle separation, the stocked microbeads were diluted in the DI water with the diluted ratio of 1:15. An extra 1% (*v*/*v*) Tween 20 was added in the suspension and made particle uniform in the ultrasonic bath. The particle suspension and polymer solution were primed in the device under a same pump. For fluorescent particle, Nikon B-2A fluorescent attachment was used while non-fluorescent ones phase contrast mode was used. In both case, a 10× objectives (NA 0.25) was used. The particles trajectories were recorded by the CCD camera for later study.

3.6 Cell separation and cell viability test

To obtain dissociated mixed cultures from the spinal cord, a method modified by Svenningsen et al. was used (Fex Svenningsen et al. 2003). The cell cultures were prepared

from embryonic stage E17 under sterile conditions. Pregnant female rat were sacrificed by an overdose of CO_2. The uterus were surgically removed from the adult rat and placed in a 100 mm Petri dish with cold Leibovitz's L-15 medium. Spinal cords were isolated from embryos and transferred to a new dish containing sterile L-15 medium and kept on ice. Dorsal root ganglia were carefully removed one by one under a dissection microscope to minimize contamination with cells from the peripheral nervous system.

The spinal cords were rinsed from meninges and cut in small segments. The tissue was mechanically dissociated through a glass Pasteur pipette until all large fragments had disappeared. Dissociated cells were washed in L-15 and centrifuged at 800–1,000 rpm to remove debris. The cells were then re-suspended in L-15, kept on ice and prepared for separation.

After surface treatment, the devices and solutions were sterilized at 120°C steam for 25 min. The syringes and tunings were flushed using 75% methanol. To keep the isoosmotic environment for cells, 3% polymer (~150 mM Na^+) was used in the cell separation. All separation procedures were performed under sterile conditions in a fume hood.

Total and viable cell counts were determined by direct microscopic counting, using Trypan Blue (Sigma-Aldrich, Sweden) staining and observation in Bürker chamber. A viability test was performed before and after separation procedures by mixing 10 μL of 0.4% solution of Trypan Blue with 10 μL solution containing cells. Cells viability was estimated due to ratio of total cells count to Trypan Blue positive (dark blue) dead cells count.

The study was approved by the regional ethics committee for research on animals in Uppsala (Sweden) and carried out in accordance with the policy of the Society for Neuroscience.

4 Results and discussion

Figure 3 shows the width faction measured for the DI-water. A clear trend is the width fraction of the polymer solution will decrease with the flow rate. The decrease velocity is larger at lower flow rate. With the extension of the flow rate, the velocity has a trend to become zero. That is, the viscosity shows a constant value with no visco-elasticity. Further more, a nonlinear phenomenon was found when the polymer solution was used at different flow rate ratios; the width fraction ratio was not equal to the flow rate ratio expected from Newtonian fluid (Wu and Nguyen 2005). The actual value was less than the flow rate ratio.

Particle separation was demonstrated at different flow rates, Fig. 4. When the flow rate of the sample flow is 5 μl/h, a clear separation was observed. When the flow rate is increased to 10 μl/h, small part of 1.9 μm particles were mixed with 9.9 μm particles. When the flow rate was increased to 20 μl/h, a large part of the smaller particle comes out with larger particles. And when the flow rate is increased to 30 μl/h, only a small part of the smaller particles is collected in the collector 1. Also, to simulate the cells separation demonstrated in this work, separation between 4.6 μm (glial cell) and 20 μm (neuron cell) particle are shown in Fig. 5.

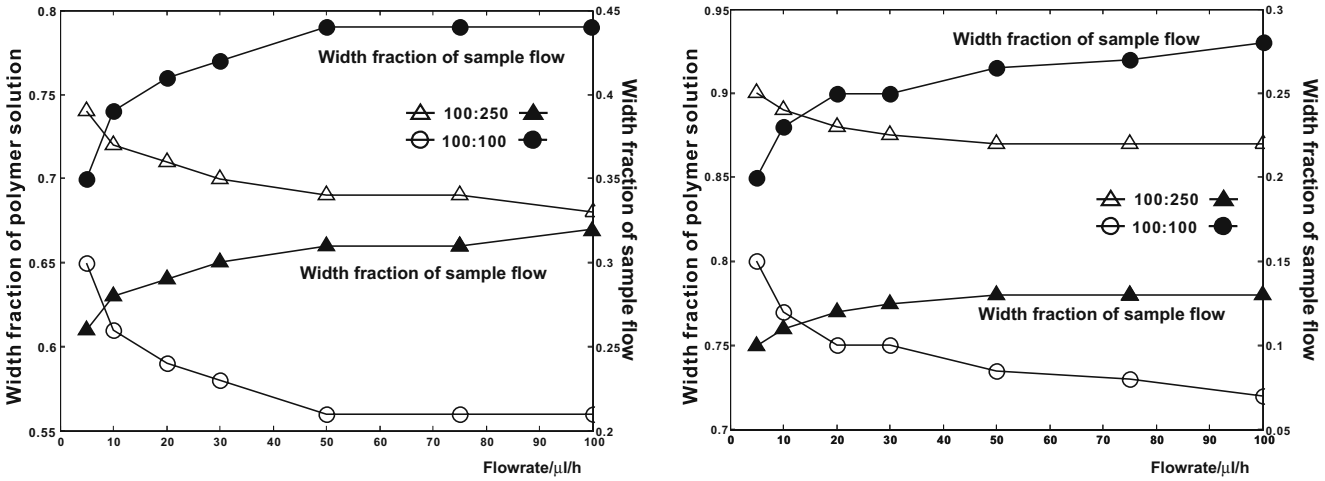

Fig. 3 Width fraction versus flow rate at different flow rate ratio of the polymer: (**a**) comparison of fraction at 100:250 (sample solution: polymer solution) and 100:100 when the polymer solution concentration is 1%; (**b**) comparison of fraction at 100:250 and 100:100 when the polymer solution concentration is 3%. Note: the filled symbols refer to the fraction of the sample flow, whereas the empty symbols refer to the fraction of the elution flow (polymer solution)

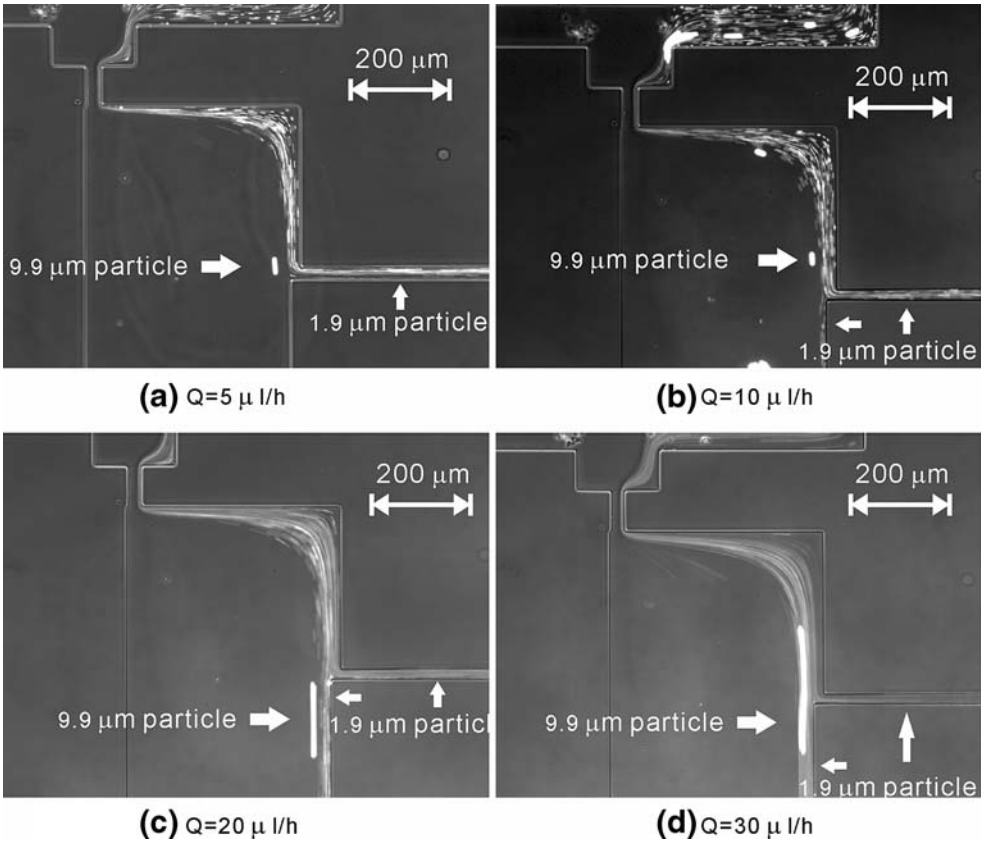

Fig. 4 Separation of particles of 1.9 and 9.9 μm sizes at different flow rate of sample flow: (**a**) Q=5μl/h; (**b**) Q=10μl/h; (**c**) Q=20μl/h and (**d**) Q=30μl/h. Both of the sample flow and elution flow is primed into the channel using the same syringe pump, with the syringe size of 100 μl and 250 μl, respectively. The Reynolds numbers at the throat are estimated to be 0.039, 0.086, 0.189 and 0.311, respectively. The exposure time are approximately 8.7, 3.0 10.8 and 12.2 ms, respectively

The separation of neural cells and glial cells is shown in Fig. 6. In the microscope, the neuron cells were found to come into the elution polymer clear. However, it is difficult to clearly see the glial cells, but they show different refractive index to the other flow, where we can see a clear interface between the original flow and elution flow.

Since neural cells are very sensitive, comparative experiments were carried out to verify our technique, Fig. 7. Figure 7(a) shows the Trypan Blue dyed cells when received and Fig. 7(b) shows them after being separated. The counting indicates the live and dead cell ratio initially is 6:7 and after separated process the ratio is about 4:5. Hence, the relative cell viability is 4:5/6:7 (~93%).

In the microfluidics, when two fluids are primed in the co-axis channel, competition between the two fluids will happen. Assumptions of the continuous velocity and the viscous rate, the spreading will be determined by the viscosity and flow rate together in the rectangular cross section channel (Wu and Nguyen 2005). According to this: When the two fluids have the same flow rate, the fraction of width of channel fluid occupied is only determined by the viscosity (exactly, the width faction of the fluid will be

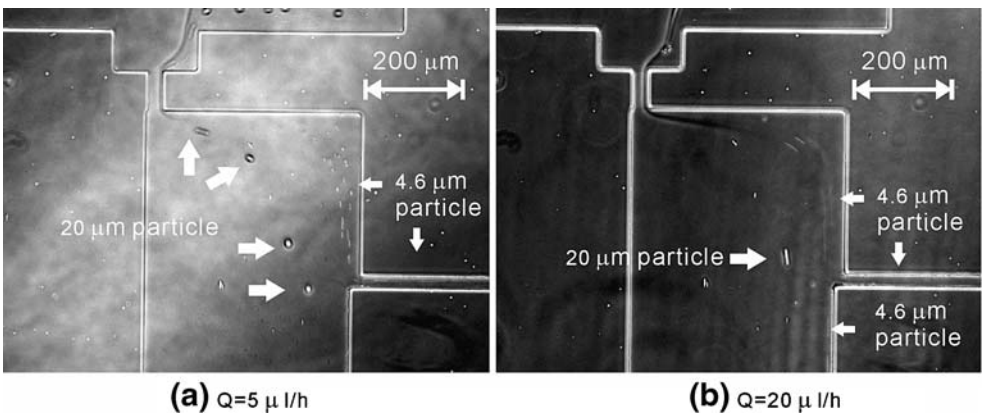

Fig. 5 Separation of particles of 4.6 and 20 μm sizes at different flow rate of sample flow: (**a**) Q=5μl/h and (**b**) Q=20μl/h. Both of the sample flow and elution flow is primed into the channel using the same syringe pump, with the syringe size of 100 μl and 250 μl, respectively. The Reynolds numbers at the throat are estimated to be 0.039 and 0.189, respectively. The exposure time are approximately 2.0 and 2.3 ms, respectively

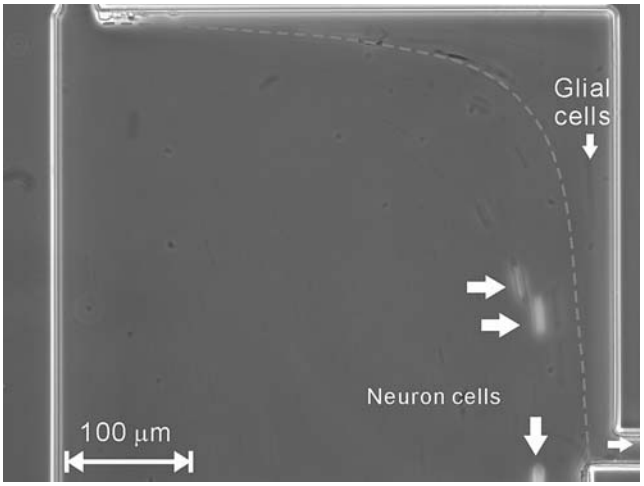

Fig. 6 Separation of neuron cells from glial cells. The Reynolds number at the throat is estimated to be 0.039. The exposure time is approximately 21.4 ms

proportional to its viscosity); when the two fluids have same viscosity, the width fraction is determined by the flow rate. Considering the 1% polymer concentration, Fig. 3(a), the width fraction with a syringe size ratio of 100:250 (sample solution: polymer solution) is higher than that with a syringe size ratio of 100:100, but the ratio is far lower the expected 2.5 (250:100). These phenomena also can be found in 3% polymer concentration, Fig. 3(b). If we compare the sample and polymer solution ratio, such as 100:100, in Fig. 3(a) and Fig. 3(b), the width fraction ratio is far smaller than the viscosity ratio. For example, at a flow rate of 5 μl/h, we can deduce that the relative viscosities to water are 1.86 (syringe size ratio of 100:100) and 4.00 (syringe size ratio of 100:250) while the width fractions of polymer are 0.65 and 0.80. Obviously, 0.80/0.65 is far smaller than 4.00/1.86. We assume that there is a nonlinear relation between the viscosity ratio and the channel fraction, which directly comes from the viscoelastic feature of polymer solution.

For the cell separation, it is more interesting to study the width fraction of the sample flow. They are complementary curves to the polymer solutions'. The width fraction of the sample flow becomes larger with the flow rate. Combination of Fig. 3(b) and Fig. 4, we show that the separation is very sensitive to the sample width fraction. In Fig. 4(a)–(d), the sample width fraction varies only little, i.e., being 0.10, 0.11, 0.12 and 0.13, respectively. However, the separation changes significantly, from clear separation (separated close to or at 100%), Fig. 4(a), to large part separation (~12.5% of the smaller particles with the larger ones), Fig. 4(b), to small part separation (~40% of the smaller particles with the larger ones), Fig. 4(c) to nearly no separation (~95% of the smaller particles with the larger ones), Fig. 4(d). At the smaller sample width fraction, we can get higher separation but suffers lower throughput. In Fig. 5, because of large particle size (20 μm), it shows larger separation distance from the smaller, a larger width fraction of sample flow can be used. With the same flow rate as for the smaller particles we collected the separated particles only from a small width fraction [Fig. 5(a)]. By increasing the flow rate we could collect the separated particles from a larger sample width fraction, Fig. 5(b). Here, tuning became very important to find the optimal operation parameters or adapt to the variation of the geometry of devices or particle sizes.

As mentioned above, the tuning can be achieved in a continuous mode. Thus, a smooth adjustment can obtained using this method. This tuning is very eased in operation, since only the flow rate is regulated without introducing any other external force or field that may be harmful to cells. In addition, using a highly viscous low-cost solution, the required elution flow volume will be much less, which may be of interest if considering future commercialization. Through a deeper channel (164 μm), a four-times-higher throughput (20 μl/h) could be achieved. In our experiments, at the typical cell concentration 1.5×10^6/ml, the corresponding throughput is 3×10^4/h, which is higher than most of microfluidic separation systems (Pamme 2007; it

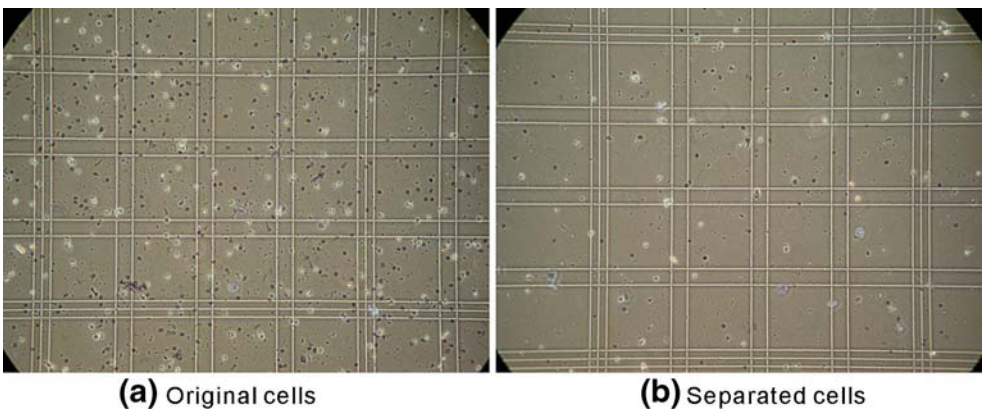

Fig. 7 Trypan Blue dyed cells: (**a**) original cells and (**b**) separated cells

should be said that further pre-concentration of these cells hamper their proliferation). Normally, the viscosity of polymer becomes larger with the extension the molecular chain. In this work, a low viscosity polymer was used, which keeps us a broad space to increase the viscosity as well as stratified the isoosmotic environment for cells.

Our novel technique based on microfluidics make possible to separate neural cells with high viability suitable for further *in vitro* study of specific cell populations. In prospective microfluidic sorting of embryonic rat neural stem cells, neuronal and glial progenitors may be applied for replacement therapy in many neurodegenerative disorders (Parkinson's disease, multiple sclerosis, amyotrophic lateral sclerosis (ALS), Alzheimer's, AIDS CNS regeneration, and cancer; Chang et al. 2007; Hedlund et al. 2007; Korecka et al. 2007).

5 Conclusions

Viscoelastic aqueous polymer solutions can be used to tune the hydrodynamic spreading, and further particle and cell separation. With this simple tuning mechanism (by only adjusting the flow rate), it provides a useful tool for the biological and medical community. Especially, inhering from a highly biocompatible polymer solution, the high cell viability of the sensitive neural cells indicates a high potential in cell study and replacement therapy.

Acknowledgements This work was partly funded by the Swedish Research Council for Environment, Agricultural Sciences and Spatial Planning, through the Uppsala Microbiomics Centre. The work was also supported by the Swedish Science Foundation for Medicine, Gyllenstiernska Krapperupstiftelsen, Åhlens and Magnus Bergvalls stiftelser and Socialstyrelsen.

References

M.T. Blom, E. Chmela, R.E. Oosterbroek, R. Tojssen, A. van den Berg, Anal. Chem. **75**, 6761 (2003)
T. Braschler, R. Johann, M. Heule, L. Metref, P. Renaud, Lab. Chip. **5**, 553 (2005)
Y.C. Chang, W.C. Shyu, H. Li, Cell. Transplant. **16**, 171 (2007)
S. Choi, S. Song, C. Choi, J.-K. Park, Lab. Chip. **7**, 1532 (2007)
S.F. Davies, J. Hood, A. Thomas, B.A. Bunnell, Stem. Cells. Dev. Apr. **15**, 191 (2006)
S.B. Devarakonda, J. Han, C.H. Ahn et al., Microfluid. Nanofluid. **3**, 391 (2007)
P.S. Dittrich, A. Manz, Nat. Rev. Drug. Discov. **5**, 210 (2006)
P.S. Dittrich, P. Schwille, Anal. Chem. **75**, 5767 (2003)
J. El-Ali, P.K. Sorger, K.F. Jensen, Nature **442**, 403 (2006)
Å. Fex Svenningsen, W.S. Shan, D.R. Colman, L. Pedraza, J. Neurosci. Res. **72**, 565 (2003)
A.Y. Fu, C. Spence, A. Scherer, F.H. Arnold, S.R. Quake, Nat. Biotechnol. **17**, 1109 (1999)
H.Y. Gan, Y.C. Lam, N.T. Nguyen, Appl. Phys. Lett. **88**, 224103 (2006)
J.C. Giddins, Science **260**, 1456 (1993)
E. Hedlund, J. Pruszak, A. Ferree, A. Vinuela, S. Hong, O. Isacson, K.S. Kim, Stem Cells **25**, 1126–35 (2007)
L.R. Huang, E.C. Cox, R.H. Austin, J.C. Sturm, Science **304**, 987 (2004)
D. Huh, A.H. Tkaczyk, J.H. Bahng, Y. Chang, H.-H. Wei, J.B. Grotberg, C.-J. Kim, K. Kurabayashi, S. Takayama, J. Am. Chem. Soc. **125**, 14678 (2003)
X.Y. Jiang, S.L. Fu, B.M. Nie, Y. Li, L. Lin, L. Yin, Y.X. Wang, P.H. Lu, X.M. Xu, J. Neurosci. Methods **158**, 13–8 (2006)
Y. Kang, D. Li, S.A. Kalams, J.E. Eid, Biomedical Microdevices (in press, DOI 10.1007/s10544-007-9130-y, 2007)
J.A. Korecka, J. Verhaagen, E.M. Hol, Regen. Med. **2**, 425 (2007)
K. Kurabayashi, S. Takayama, J. Am. Chem. Soc. **125**, 14678 (2003)
A.M. Leshansky, A. Bransky, N. Korin et al., Phys. Rew. Lett **98**, 234501 (2007)
N. Pamme, Lab. Chip. **7**, 1644 (2007)
N. Pamme, C. Wilhelm, Lab. Chip. **6**, 974 (2006)
F. Petersson, A. Nilsson, C. Holm, H. Jonsson, T. Laurell, Lab. Chip. **5**, 20 (2005)
J.C. Sanders, M.C. Breadmore, Y.C. Kwok, K.M. Horsman, J.P. Landers, Anal. Chem. **75**, 986 (2003)
T.M. Squires, S.R. Quake, Rev. Mod. Phys. **77**, 977 (2005)
J. Takagi, M. Yamada, M. Yasuda, M. Seki, Lab. Chip **5**, 778 (2005)
W.J. Wang, X.H. Wang, Q.L. Feng, F.Z. Cui, Y.X. Xu, X.H. Song, J. Bioact. Compat. Pol. **18**, 249 (2003)
Z.G. Wu, N.T. Nguyen, Sensors Actuators B **107**, 965 (2005)
Z.G. Wu, N.T. Nguyen, X.Y. Huang, J. Micromech. Microeng. **14**, 604 (2004)
Z.G. Wu, A.Q. Liu, K. Hjort, J. Micromech. Microeng. **17**, 1992 (2007)
Y. Xia, G.M. Whitesides, Annu. Rev. Mater. Sci. **28**, 153 (1998)
M. Yamada, M. Nakashima, M. Seki, Anal. Chem. **76**, 5465 (2004)
M. Yamada, K. Kano, Y. Tsuda, J. Kobayashi, M. Yamato, M. Seki, T. Okano, Biomed. Microdev. **9**, 637 (2007)
S. Yang, A. Ündar, J.D. Zahn, Lab. Chip. **6**, 871 (2006)
Y.H. Zhang, R.W. Barber, D.R. Emerson, Curr. Anal. Chem. **1**, 345 (2005)